20th IMEKO TC4 International Symposium and
18th International Workshop on ADC Modelling and Testing
Research on Electric and Electronic Measurement for the Economic Upturn
Benevento, Italy, September 15-17, 2014

Advanced measurements on cantilever retaining wall models during earthquake simulations

Augusto Penna[1], Anna Scotto di Santolo[2], Panos Kloukinas[3], Colin A. Taylor[3], George Mylonakis[3], Aldo Evangelista[4], Armando L. Simonelli[1]

[1] *University of Sannio, Dep. of Engineering, Piazza Roma, 27-1, 82100 Benevento, IT, aupenna@unina.it , alsimone@unisannio.it*

[2] *Pegaso University, Piazza Trieste e Trento, 48, 80132 Napoli, IT, anscotto@unina.it*

[3] *University of Bristol, Dep. of Civil Engineering, University Walk, Clifton BS8 1TR, Bristol, UK p.kloukinas@bristol.ac.uk, colin.taylor@bristol.ac.uk, g.mylonakis@bristol.ac.uk*

[4] *University of Naples Federico II, DICEA Department, via Claudio 21, 80125 Napoli, IT evangeli@unina.it*

A. Introduction

Reinforced concrete cantilever retaining walls represent a popular type of retaining system. It is widely considered as advantageous over conventional gravity walls as it combines economy and ease in construction and installation. The concept is deemed particularly rational, as it exploits the stabilizing action of the soil weight over the footing slab against both sliding and overturning, thus allowing construction of walls of considerable height. Nevertheless, the issue of seismic behavior remains little explored. In fact many modern Codes, including the Eurocodes (Eurocode8-Part 5, 2003 [1]) and the Italian Building Code (NTC, 2008 [2]), do not explicitly refer to cantilever walls.

Based on the recent theoretical findings (Kloukinas & Mylonakis, 2011 [3]; Evangelista et al., 2010 [4]) a series of shaking table tests were designed and conducted at the 6-DOF Earthquake Simulator of the Earthquake and Large Structures Laboratory (EQUALS) at the University of Bristol, UK.

The aim of the experimental investigation is to better understand the soil-wall dynamic interaction problem, the relationship between design parameters, stability safety factors and failure mechanisms, and the validation of the seismic Rankine theoretical model. Details on the experimental hardware, materials, configurations and procedure are provided in the ensuing.

B. Principles of Physical Modelling

The desired modelling outcomes and the capabilities and the limitations of the existing test facilities are driving factors in the modelling activity. The scale factors for single gravity models are shown in Table 1.

The model cantilever walls tested in this study have the simplified geometry shown in Figure 1. Two sizes of heel width (B) were considered in design ('long heel wall' and 'short heel wall'). For the 'long heel wall', the Rankine stress characteristics fully develop in the soil without intersecting the wall, while for the 'short heel wall' the Rankine stress characteristics intersect the body of the wall. The model wall height is the reference dimension governing the physical modelling of the cantilever wall and the enclosing container.

The physical modelling activity has explored two candidate solutions for the scaled wall model: Model A (height *H=600 mm*) and Model B (height: *H=1000 mm*). The proposed models are based on a concrete wall prototype of height *H=5400 mm* and base *B=3000* mm. Therefore the resulting scaling factors for Model A and Model B are SF=9 and SF=5.4, respectively. Figure 1 presents the geometry of both prototype and models.

The dimensions of the required supporting layer that allow unrestricted spreading of loads in the base will dictate the dimensions of the enclosing container. The maximum dimensions of the enclosing container are limited by the size of the shaking table.

A summary of the design calculations is presented in Table 2.

ISBN-14: 978-92-990073-2-7

Table 1 - Scale factors for single gravity models (Wood et. al, 2002[5])

Variable	Scale Factor	Magnitude
Length	$Length_{model}$ / $Length_{prototype}$ = n_l	1/n
Density	n_ρ	1
Stiffness	n_G	$1/\sqrt{n}$
Acceleration	n_g	1
Stress	$n_\rho n_g n_l$	1/n
Strain	$n_\rho n_g n_l / n_G$	$1/\sqrt{n}$
Displacement	$n_\rho n_g n_l^2 / n_G$	$1/n^{1.5}$
Velocity	$n_g n_l \sqrt{(n_\rho/n_G)}$	$1/n^{0.75}$
Dynamic time	$n_l \sqrt{(n_\rho/n_G)}$	$1/n^{0.75}$
Frequency	$\sqrt{(n_G/n_\rho)}/n_l$	$n^{0.75}$
Shear wave velocity	$\sqrt{(n_G/n_\rho)}$	$1/n^{0.25}$

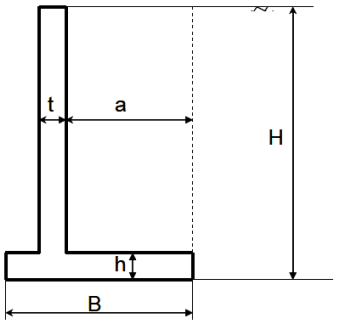

Unit Measure	Notation	PROTOTYPE	MODEL A	MODEL B
		concrete	dural (SF=9)	dural (SF=5.4)
m	H	5.40	0.60	1.00
m	B	3.00	0.33	0.56
m	t	0.30	0.03	0.06
m	h	0.40	0.04	0.07
m	a	1.75	0.19	0.32

Fig. 1. Simplified Geometry of Cantilever Wall. Dimensions for Prototype and Proposed Wall Models.

By comparing the calculation results for Model A and Model B, it is considered that Model A was the best solution for the model wall.
Two model walls were manufactured: Model A.1 ('long heel wall') and Model A.2 ('short heel wall').
The two model walls were strain gauged and their bending response was monitored.

C. Shaking table model geometry and instrumentation

The model geometry adopted in the design, shown in Figure 2, had to take into consideration the container dimensions, and the restrictions of the shaking table regarding the maximum payload. A maximum soil height of 1m was selected, corresponding to a backfill of 0.6m (equal to the wall height, H) and the foundation soil layer of 0.4m (equal to wall footing width, B). The length of the retained backfill was selected at 5 times its height, whereas the corresponding free length in the front of the wall was 3 times the wall height. These distances were deemed sufficient to eliminate the boundary effects and to ensure free field conditions.
Three types of instruments were employed for the measurement of accelerations, displacements and strains as shown in Figure 2a and described in Table 3. 21 1-D accelerometers were used to monitor the motion of the shaking table, the shear stack and the wall-soil system, with the main area of interest being the wall itself, the retained soil mass and the free field. 4 LVDT transducers were used to measure the transient and permanent displacements of the wall. Additionally, 32 strain gauges were attached on the stem and the base of the wall, on three cross sections, to monitor the bending of the wall.

Table 2 - Design Calculations: Prototype, Model A and Model B

Variables:	Unit Measure	Notation	PROTOTYPE concrete	MODEL A dural (SF=9)	MODEL B dural (SF=5.4)
Wall height	m	H	5.40	0.60	1.00
Wall base	m	B	3.00	0.33	0.56
Wall thickness	m	t	0.30	0.03	0.06
Heel height	m	h	0.40	0.04	0.07
Distance between stem and heel	m	a	1.75	0.19	0.32
Packing density of backfill	kg/m3	r1	1400.00	1400.00	1400.00
Unit weight of backfill	N/m3	g1	13734.00	13734.00	13734.00
Unit weight of wall material (concrete, aluminium)	N/m3	gw	23500.00	26977.00	26977.00
Cohesion in backfill		c	0.00	0.00	0.00
Angle of internal friction backfill	deg	f	34.00	34.00	34.00
Angle of friction between base and foundation soil	deg	f'	27.00	27.00	27.00
Tangent of angle of friction between base and found.			0.51	0.51	0.51
Coefficient of active pressure		Ka	0.26	0.26	0.26
Active thrust (horizontal force due to backfill)	N/m	Pa	52062.85	642.75	1785.42
Passive resistance	N/m	Pv			
Surcharge (suprastructure)	N/m	L	0.00	0.00	0.00
Horizontal force due to surcharge	N/m	Lh	0.00	0.00	0.00
Total Horizontal Force on Base	***N/m***	***Rh***	***52062.85***	***642.75***	***1785.42***
Resultant horizontal moment about toe	***Nm***	***Mh***	***93713.12***	***128.55***	***595.14***
Weight of stem	N/m	Ws	35250.00	499.57	1387.71
Weight of base	N/m	Wb	28200.00	399.66	1110.16
Weight of soil	N/m	Ws	120172.50	1483.61	4121.14
Weight surcharge	N/m	Lv	0.00	0.00	0.00
Total Vertical Force on Base	***N/m***	***Rv***	***183622.50***	***2382.84***	***6619.01***
Moment of stem weight abt toe	Nm	M1	38775.00	61.06	282.68
Moment of base weight abt toe	Nm	M2	42300.00	66.61	308.38
Moment of soil weight abt toe	Nm	M3	255366.56	350.30	1621.75
Moment of weight surcharge abt toe	Nm	M4	0.00	0.00	0.00
Resultant vertical moment about toe	***Nm***	***Mv***	***336441.56***	***477.97***	***2212.81***
Resultant moment about toe	***Nm***	***M***	***242728.44***	***349.42***	***1617.67***
Lever arm of base resultant	m	l	1.32	0.15	0.24
Eccentricity of base reaction	m	e	0.18	0.02	0.03
Check that e < B/6 (to avoid tensile stress at heel)	***m***	***B/6***	***0.50***	***0.06***	***0.09***
Maximum base pressure (at the toe)	N/m2	pmax	83011.04	9725.68	16209.47
Minimum base pressure(at the heel)	N/m2	pmax	39403.96	4571.38	7618.97
Factor of safety against sliding		***FSL***	***1.80***	***1.89***	***1.89***
Check for bearing capacity failure					
Depth of wall inside supporting layer	m	D	0.80	0.09	0.15
Packing density of supporting layer	kg/m3	r2	1900	1900	1900
Unit weight of supporting layer	N/m3	g2	18639	18639	18639
Angle of internal friction base soill	deg	f2	42.00	42.00	42.00
Factor for soil weight contribution (Meyerhof factor)		Ng	262.74	262.74	262.74
Factor for contribution of surcharge (Meyerhof factor)		Nq	134.87	134.87	134.87
Ultimate bearing capacity footing	N/m2	qu	935688.983	103965.443	173275.738
Factor of safety for bearing capacity		***FS***	***11.272***	***10.690***	***10.690***

(a)

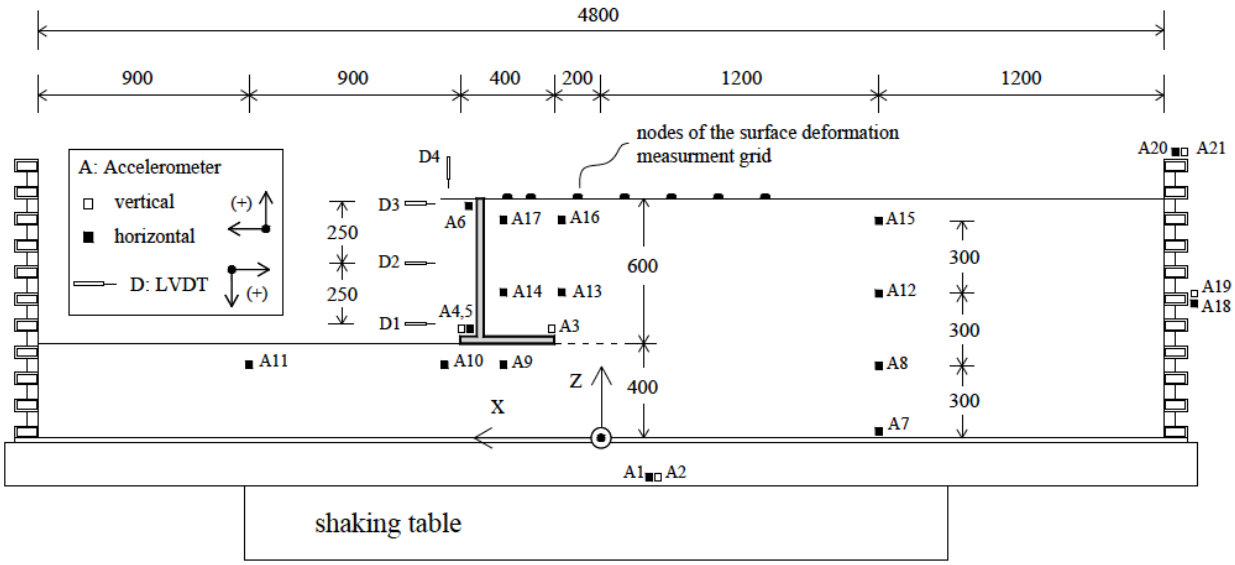

(b)

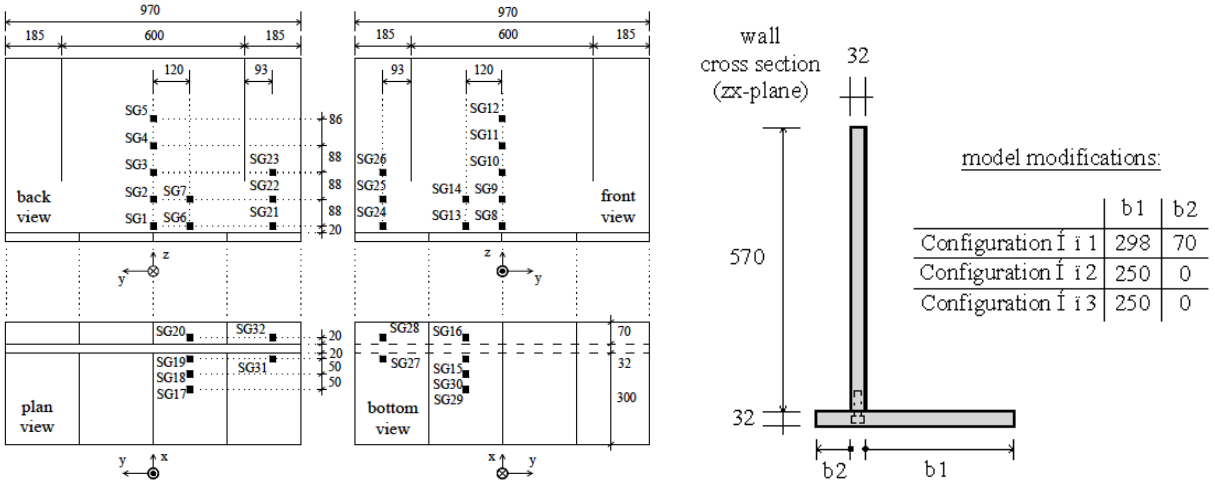

Fig. 2 – a) Geometry and instrumentation of the shaking table model; b) Wall model geometry and positions of strain gauges (dimensions in mm)

Table 3 – Instrumentation summary

Measured Parameter	Transducer Type	Description	Purpose
Strain	Strain gauge type EA-13-120LZ-120 (Vishay Ltd)	Linear strain gauge pattern, 3 mm length	Used to measure bending strain of wall at various elevations (on Y direction).
Acceleration	Accelerator type: SETRA 141A	High output capacitance type sensor with inbuilt pre-amplifier. Calibrated range: +/-8g. Operating frequency: 0-3000 Hz	Used to measure: -the Y/Z accelerations of the box at various ordinates -the Y/Z acceleration of the wall at various ordinates -the Y acceleration of the backfill at various ordinates
Displacement	Type RDP DCTH LVDT	Linear variable displacement transformer	Used to monitor the H/V displacement of the wall at various ordinates.
	Type INDIKON	Non-contact displacement transducer. Operation based on eddy effect.	Used to monitor the displacement of the free surface of the backfill. The transducers will be attached to plates resting on a Perspex pad with roughened base.

Lastly, non-contact displacement transducers were employed to monitor the backfill settlement, but proved to be inefficient due to low operational range (~10mm) and were replaced by a grid of coloured sand.
The retaining wall model, depicted in Fig 2b, was made of aluminium alloy 5083 plates with properties: unit weight γ=27 *kN/m3*, Young's modulus *E*=70*GPa*, Poisson's ratio n=0.3.
Both the backfill and the foundation soil layer consisted of dry, yellow Leighton Buzzard (LB) silica sand, 14–25 (Fraction B) with properties *Dmin=0.6mm, Dmax=1.18 mm, D50=0.82 mm, Gs=2.64 Mg/m3, emin=0.486, emax=0.78*, at different compaction levels. This soil material has been used extensively in experimental research and a wide set of mechanical and dynamic properties is available (Dietz & Muir Wood, 2007 [6]). The soil configuration consists of a dense supporting layer and a medium dense backfill. The characteristics of the soil layers are summarized in Table 4.
In addition to the soil properties, the mechanical properties of the interfaces are important for the soil-wall system behaviour. Two kinds of footing interfaces were employed: a) a smooth interface of an aluminum plate and sand; b) a rough interface, created by pasting rough sandpaper on the footing surface. The interface friction angles were measured directly on the model via static pull tests. The values are: Smooth soil-wall interface: δ=23.5°; Rough soil-wall interface δ=28.5°.
Three different model configurations (No1, No2 and No3) were tested: (a) Configuration No1, corresponding to the reference geometry of Fig. 2 (*B*=400mm, *b1*=300mm, *b2*=70mm), with a smooth footing interface, (b) Configuration No2, corresponding to a shorter footing width (*B*=280mm, *b1*=250mm, *b2*=0) and (c) Configuration No3, with an identical geometry as Configuration No2, but with a rough interface, as explained above.

D. Experimental procedure

The three wall Configurations were subjected to the following series of dynamic tests: (1) Exploratory white noise testing to investigate the soil-wall system response; (2) Harmonic-sinusoidal inputs at various excitation frequencies and increasing amplitude, until yielding of the wall and sufficient plastic deformation of the system recorded; (3) Dynamic excitation of the system with scaled earthquake signals of increasing amplitude, again until sufficient yielding of the wall recorded. Note that restoration of the wall-backfill system was needed after steps 2 and 3.
During exploratory white noise testing, a random noise signal of bandwidth *1-100 Hz* and *RMS* acceleration=0.005*g* was employed. Harmonic excitation involved sine dwells consisting of 15 steady

Table 4 – Soil Properties

Soil layers	Thickness (mm)	e	D_r (%)	γ (kN/m^3)	φ(°)
Foundation	390	0.61	60	16.14	42
Backfill	600	0.72	22	15.07	34

cycles, 5-cycle ramp up to full test level at the beginning and a 5-cycle ramp down to zero at the end, to smoothen out the transition between transient and steadystate response. After dynamic investigation of the system at various excitation frequencies and low acceleration amplitude of 0.05*g*, a sole frequency of 7*Hz* was employed with increasing amplitude, until failure.
For the seismic testing, a modified version of the Sturno record from Irpinia-Italy, 1980 earthquake (*Mw*= 6.9, *PGA*=0.32*g*), was selected, characterized by a strong motion duration of 16.2*sec* and energy transfer to a wide range of frequencies from 0.1 to 3 *Hz* (fig.3). A frequency scale factor of 5 was applied to the original signal, according to scaling laws for 1-*g* conditions.
Regarding the data acquisition, the output signals were filtered with a low pass Butterworth filter of 80 *Hz* by a FERN EF6 multi-channel programmable filter and sampled at 1024 *Hz*, except of the white noise tests which were sampled at 256 *Hz*.

E. Typical results for earthquake simulation

A key experimental measurement is presented in Figure 4 with reference to dynamic and permanent displacements and bending moments. The results presented relate to Configurations 1 and 3, since they exhibit yielding for similar acceleration conditions, yet under different modes.
The input motion contains higher effective peak accelerations, but the number of important strong motion cycles (half cycle pulses) is only three.
The response of each configuration is as expected, exhibiting a consistent, repeatable, behavior with respect to yielding.

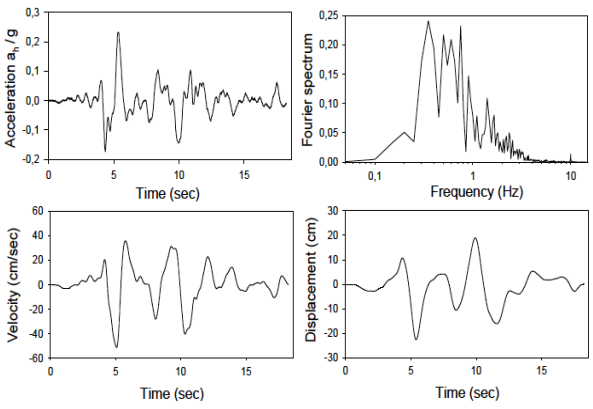

Fig. 3 – Modifies Sturno input motion.

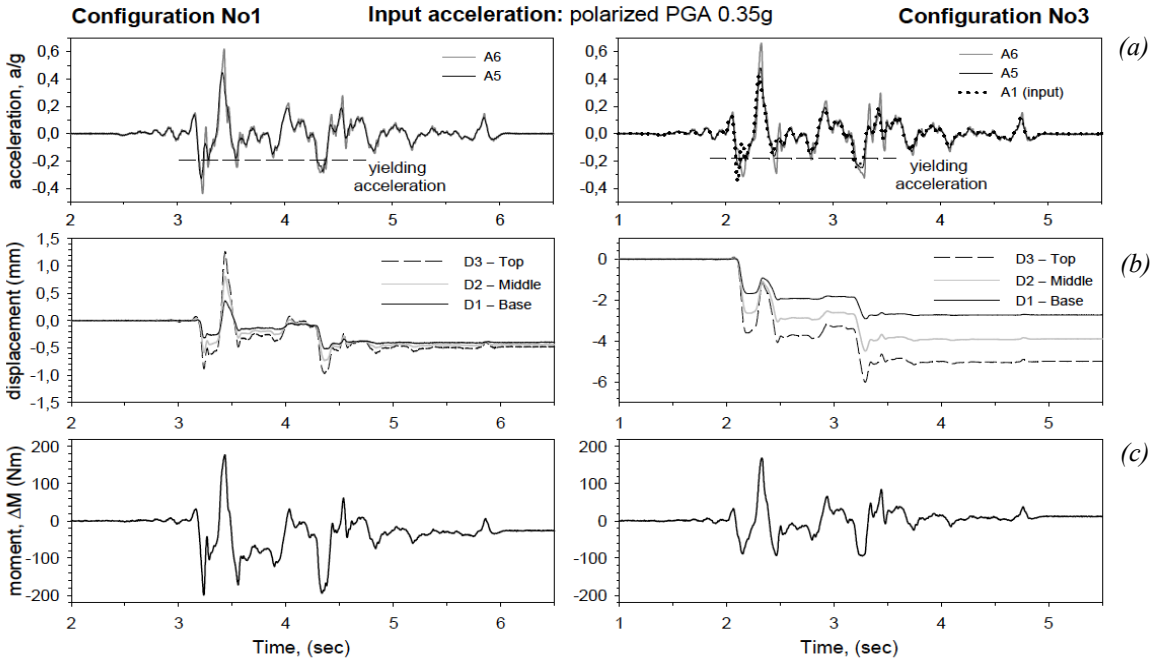

Fig. 4 – Comparison of typical experimental under seismic excitation of polarized PGA 0.35g with respect to: (a) wall accelerations, (b) wall displacements, (c) maximum dynamic moment ΔM on the cantilever wall stem

The sliding failure mode is clearly visible in Configuration 1, as is the bearing capacity failure in Configuration 3 (caused by the high eccentricities induced by seismic thrust).

An important observation is that the bending moment at the base of the stem (positive *ΔM*) increases when the wall moves towards the backfill, that is for an acceleration which is not critical for the overall stability. On the other hand, during active conditions, bending moment is minimized. It appears that when the inertial action drives the wall towards the backfill, stresses increase towards the passive state, peak bending moments develop, and the backfill exhibits a stiffer behavior.

F. Conclusion remarks

A series of shaking table tests on scaled models of cantilever retaining walls were conducted in the BLADE laboratory at the University of Bristol.

Preliminary interpretation of the experimental findings, confirms the predictions of the theoretical analysis, with reference to the failure mechanisms and the critical yield accelerations of the system. Regarding seismic loads on the structure, it is shown that the soil thrust maximizing the bending moment on the wall stem, does not coincide with the critical earth pressure for overall stability, but they appear to act at different time instances. This indicates that different load combinations have to be employed for the sizing of the wall stem and for stability analysis of the overall system against sliding and bearing capacity!

Acknowledgements

The research leading to these results has received funding from the European Union Seventh Framework Programme (FP7/2007-2013) under grant agreement n°227887, SERIES.

REFERENCES

[1] Eurocode 8, (2003). Design provisions for earthquake resistance of structures, Part 5: Foundations,retaining structures and geotechnical aspects, CEN E.C. for Standardization, Bruxelles.

[2] NTC (2008). Italian Building Code, DM 14 Jan., G.U. n. 29, 4 Feb., n. 30.

[3] Kloukinas, P. and Mylonakis, G. (2011). Rankine Solution for seismic earth pressures on L-shaped retaining walls, 5 ICEGE, Santiago, Chile, January 10-13

[4] Evangelista A., Scotto di Santolo A., Simonelli A.L. (2010). Evaluation of pseudostatic active earth pressure coefficient of cantilever retaining walls, Soil Dynamics & Earthquake Engineering, 30:11, 1119-1128.

[5] Muir Wood D., Crewe A. & Taylor C.A. (2002). Shaking Table Testing of Geotechnical Models, UPMG International Journal of Physical Modelling in Geotechnics, 2, 01-13.

[6] Dietz MS & Muir Wood D (2007) Shaking table evaluation of dynamic soil properties. Proceedings of the fourth international conference on earthquake geotechnical engineering, Thessaloniki, Greece, June 24–28.